

## Supporting information

### MOF-derived Interface-rich Silver/Silver Oxide Nano-structures as an Effective Electrocatalyst for Oxidation of 5-Hydroxymethylfurfural to 2,5-Furandicarboxylic Acid (FDCA) with Spontaneous FDCA Separation in Acid Media

Rajib Samanta,<sup>#a,b</sup> Debashish Paik,<sup>#a,b</sup> Manjunatha Kempasiddaiah,<sup>a,b</sup> Sonali Panigrahy,<sup>a,b</sup> Sudip Barman<sup>\*a,b</sup>

<sup>a</sup> School of Chemical Sciences, National Institute of Science Education and Research (NISER), HBNI, Bhubaneswar, Orissa-752050, India, Tel.: +91 6742494183.

<sup>b</sup> Homi Bhabha National Institute, Training School Complex, Anushaktinagar, Mumbai 400094, India.

# Authors of equal contribution

\*S.B.: e-mail: sbarman@niser.ac.in; Tel: +91(674)2494183.

**ORCID:** Sudip Barman: 0000-0002-4285-9417

#### Materials:

Silver (I) nitrate (AgNO<sub>3</sub>, 99+% assays), 2-methylimidazole were purchased from Sigma-Aldrich. Sulphuric acid (H<sub>2</sub>SO<sub>4</sub>, 98%) was purchased from Merck (Germany). HMF (99+% assay) was bought from Spectrochem (India). All these chemicals were used as they were received without further purification. Ar gas (99.99% purity) was bought from Sigma-Aldrich. Milli-Q water was obtained from an ultra-filtration system (Milli-Q, Millipore), and the measured conductivity was 35 mho·cm<sup>-1</sup> at 25 °C.

#### Characterizations:

Field-emission scanning electron microscope (FESEM) system (Carl Zeiss, Germany make, Model: Sigma) was used for taking FESEM images. FESEM samples were prepared by casting the dispersed sample on a Si-wafer and dried at air around 45 °C. The powder x-ray diffraction pattern (p-XRD) of samples was performed by Bruker DAVINCI D8 ADVANCE diffractometer equipped with Cu K $\alpha$  radiation ( $\lambda$ = 0.15406 nm). NMR spectra were collected

by Bruker Advance III 400 MHz NMR spectrometer. Typically, 450 micro-liters of reaction mixture and fifty micro-liters D<sub>2</sub>O mixture was used for NMR study by water suppression method. Transmission Electron Microscopy (TEM, JEOL F200) operated at 200 kV, was used to investigate surface morphology and also used to take High-Resolution TEM (HRTEM) images. For TEM sample preparation, 10 μL solutions was taken from a stock solution of 0.2 mg/mL and dried at air around 45°C. XPS measurements were done by VG Microtech where monochromatic source was Mg K $\alpha$  X-ray. XPS was taken from the sample deposited on Si wafer. All the electrochemical measurements were performed with an Electrochemical Workstation (Autolab, Metrohm, PGSTAT 302N). A three electrode system was used for the electrocatalysis; where the catalyst modified carbon cloth was used as working electrode, a graphite rod and an Ag/AgCl electrode were used as counter and reference electrode, respectively. For LSV, 10 mM HMF is added in 0.5 M H<sub>2</sub>SO<sub>4</sub> and the potential are given from 0.9 to 2.0 V (RHE). Smoothing was applied in chronoamperometric responses where needed to reduce noise in chronoamperometric measurements due to bubble accumulation. The pH of the working solution was measured before experiment using Hanna (HI 2209) pH meter.

### **Electrode Preparation:**

Carbon cloth (1 cm  $\times$  2 cm) was used as a current collector to prepare the cathode. To clean the carbon cloth, it was first washed with 2-propanol and water, and then treated with 1 M HCl for 1 minute to remove any oxide layer on the surface followed by washing with water for further use. The stock solution for HMF reduction was prepared by adding 1 mg of the catalysts to 1 mL of Millipore water and sonicated for 30 minutes. 750 μL of aqueous stock solution was drop-casted and evaporated on cleaned carbon cloth (1 cm  $\times$  1 cm) to prepare Ag/AgO<sub>x</sub>-CN<sub>x</sub> electrode.

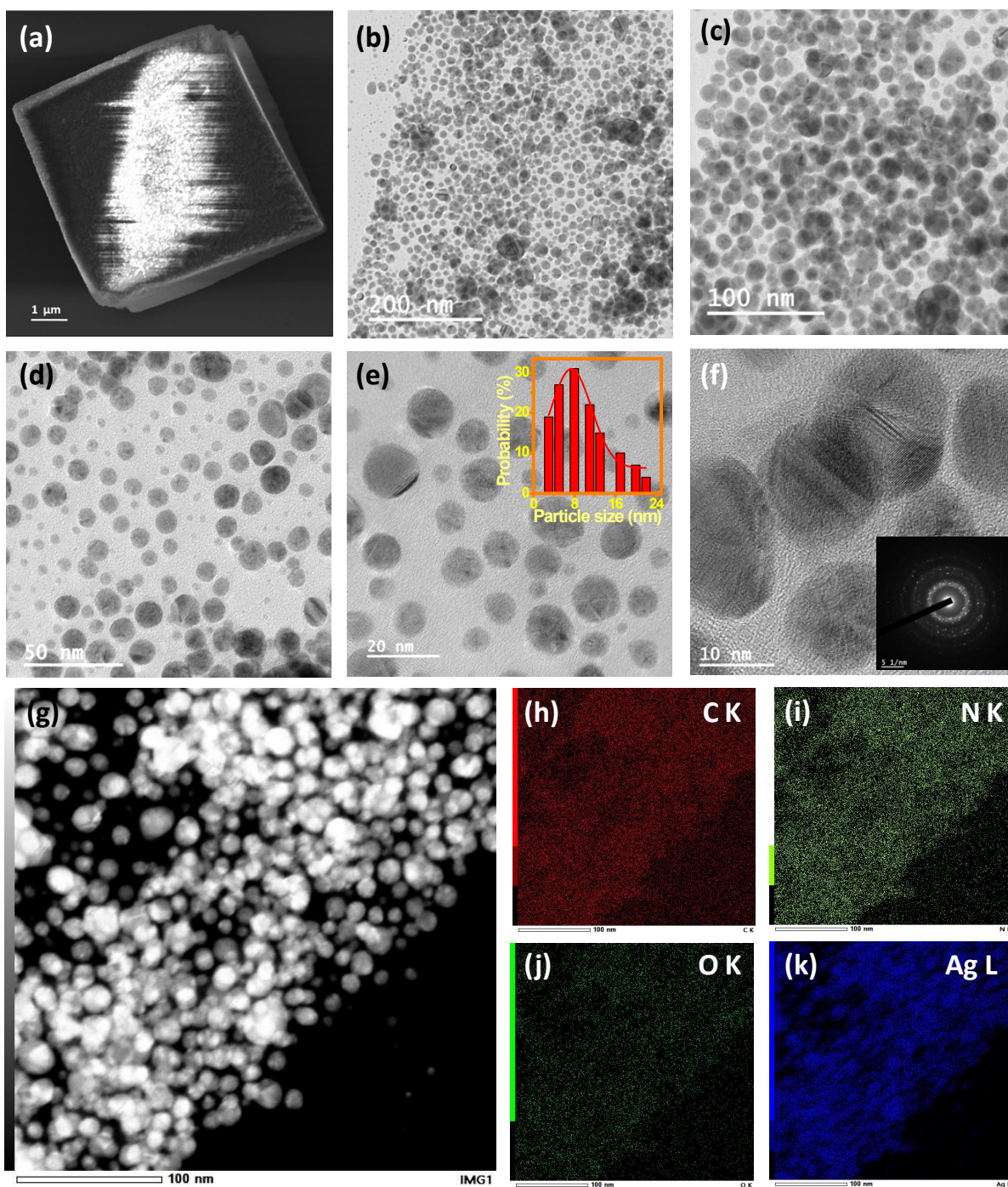


**Figure S1.** (a) FESEM image of Ag-MOF, (b-e) TEM images (inset Figure 1e: particle size distribution plot) of Ag-MOF, (f) HRTEM image (inset: SAED image) of Ag-MOF. (g-k) STEM and corresponding elemental mapping of Ag-MOF.

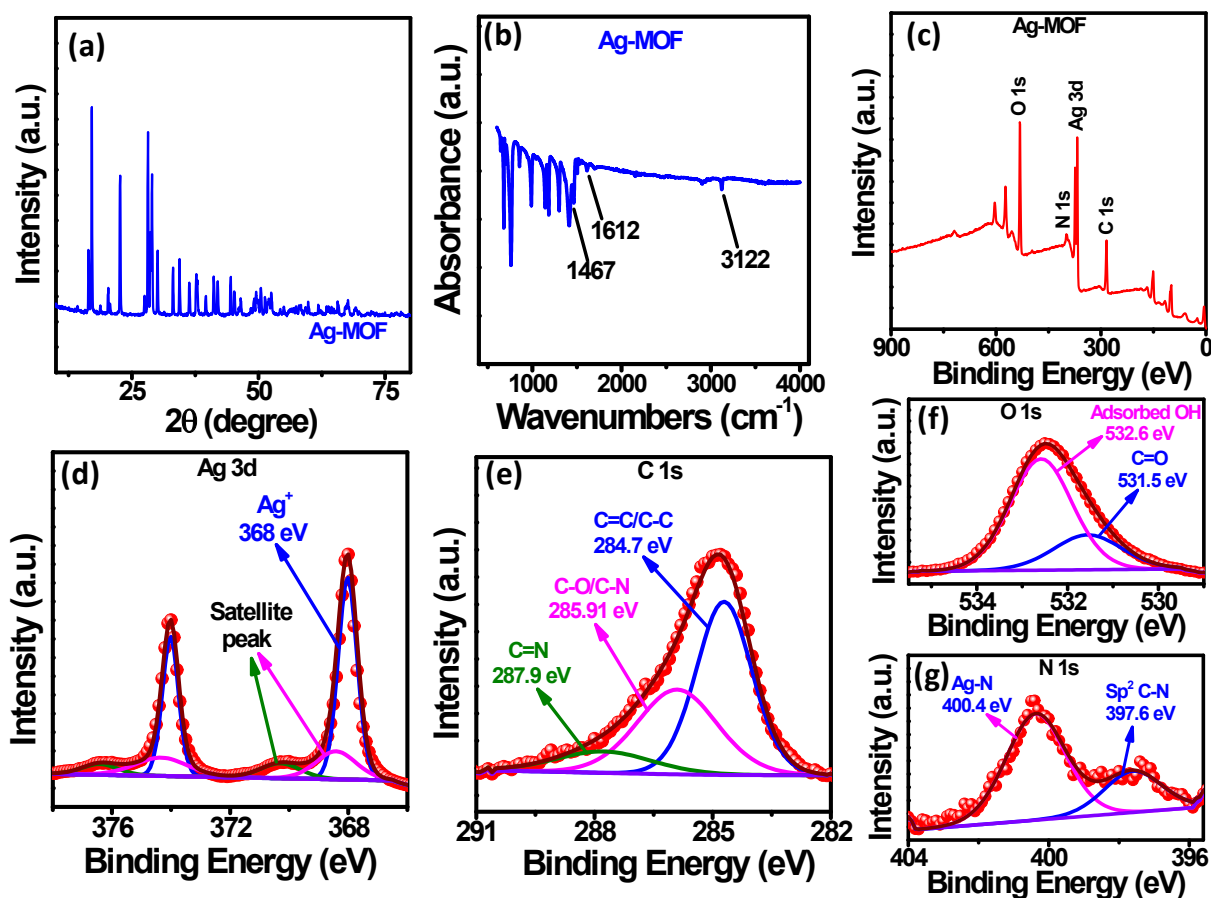


**Figure S2.** (a) p-XRD pattern of Ag-MOF; (b) ATR-FTIR spectrum of Ag-MOF; (c) XPS survey scan of Ag-MOF, (d-g) High resolution XPS spectrum of Ag 3d, C 1s, O 1s, and N 1s of Ag-MOF.

### Tafel plot:

For fitting of linear region of Tafel plots, Tafel formula:  $\eta = b \log (J) + a$ , where ‘ $\eta$ ’, ‘ $J$ ’, ‘ $b$ ’, and ‘ $a$ ’ is overpotential, current density, Tafel slope and constant respectively is used.

Where,  $b = 2.3RT/\alpha F$  ( $R$  - gas constant,  $\alpha$  - symmetry coefficient,  $T$  - absolute temperature,  $F$  - faraday constant). During the electrochemical process, the faster electron transfer indicates the lower value of the Tafel slope ( $b$ ).

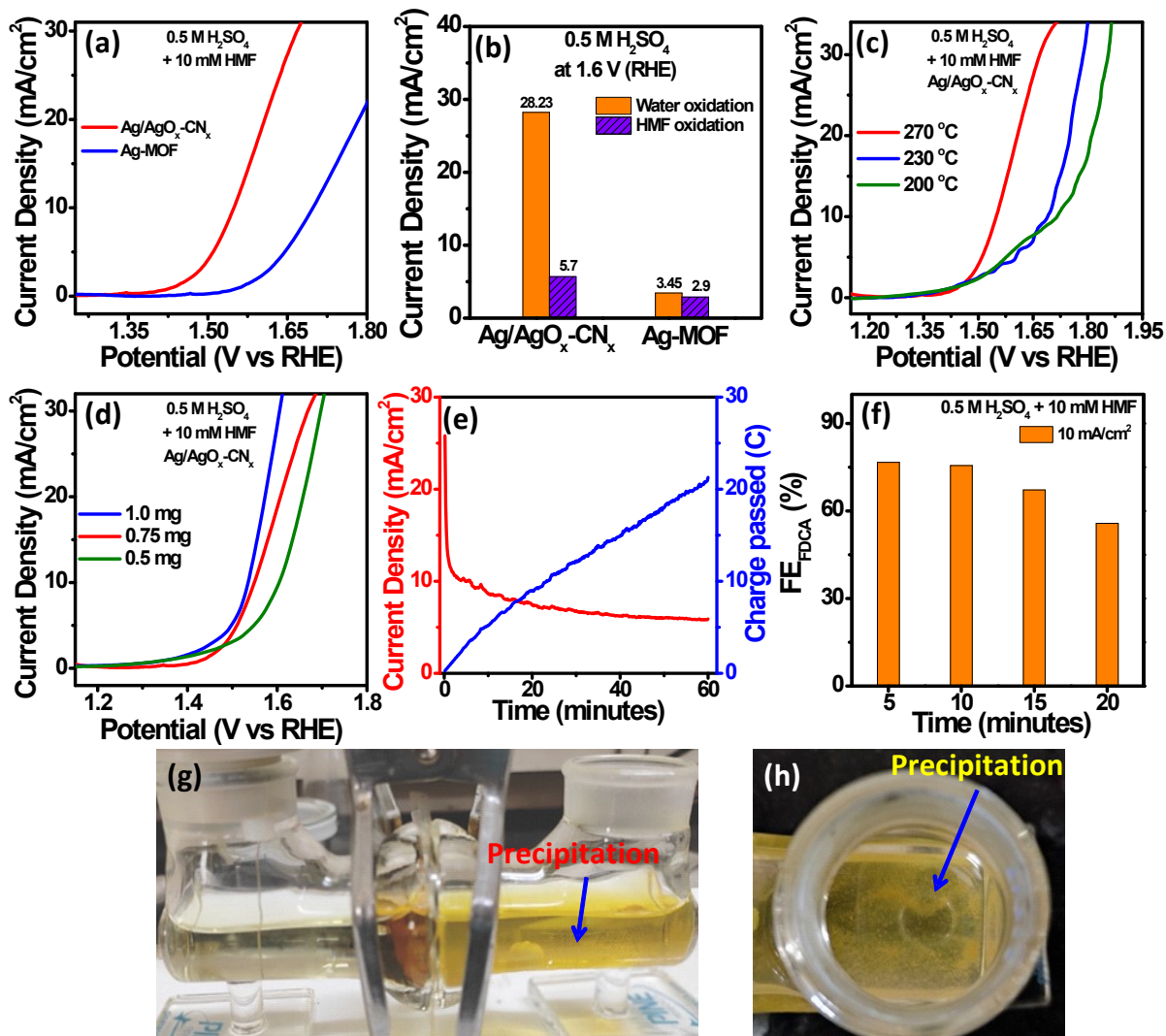


**Figure S3.** (a) Non iR-corrected HMF oxidation LSV curves of Ag/AgO<sub>x</sub>-CN<sub>x</sub>, and Ag-MOF in 0.5 M H<sub>2</sub>SO<sub>4</sub>; (b) Current densities of the catalysts at 1.6 V (RHE) during HMF and water electrolysis; (c, d) HMF oxidation LSV curves of Ag/AgO<sub>x</sub>-CN<sub>x</sub> with different synthesis temperature and different loading; (e) Current and charge versus time plot of Ag/AgO<sub>x</sub>-CN<sub>x</sub>; (f) faradic efficiency of FDCA at 10 mA/cm<sup>2</sup> current density of Ag/AgO<sub>x</sub>-CN<sub>x</sub> for different time; (g, h) Side and top view of cell setup after the reaction on 50 mM HMF solution showing the precipitation of the products.



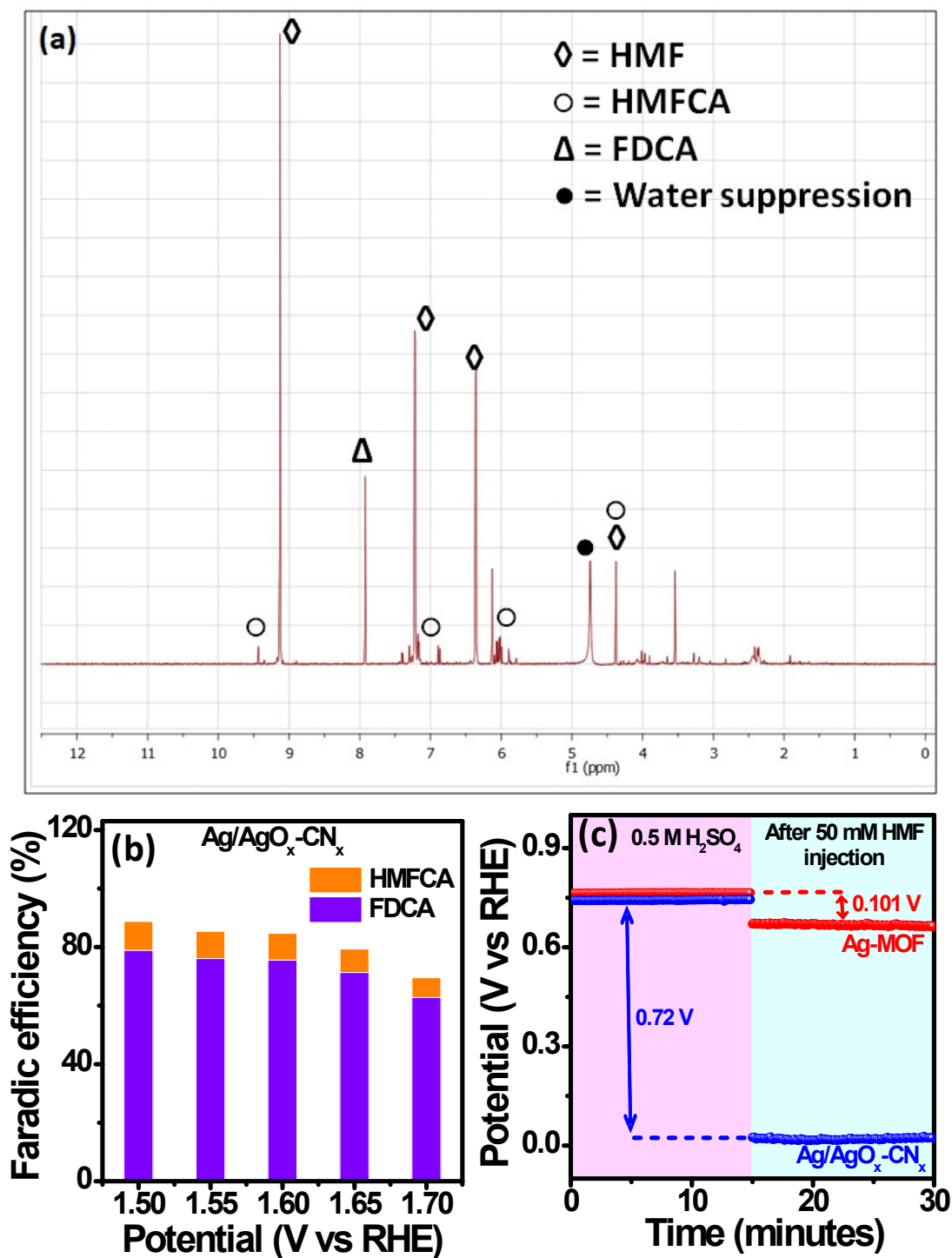


**Figure S4.** (a) NMR spectrum of the reaction mixture after 10 minutes of reaction; (b) Faradic efficiency of FDCA and HMFCAs of Ag/AgO<sub>x</sub>-CN<sub>x</sub> at different potential; (c) OCP curves of Ag/AgO<sub>x</sub>-CN<sub>x</sub> and Ag-MOF in 0.5 M H<sub>2</sub>SO<sub>4</sub> with 50 mM HMF being injected subsequently.

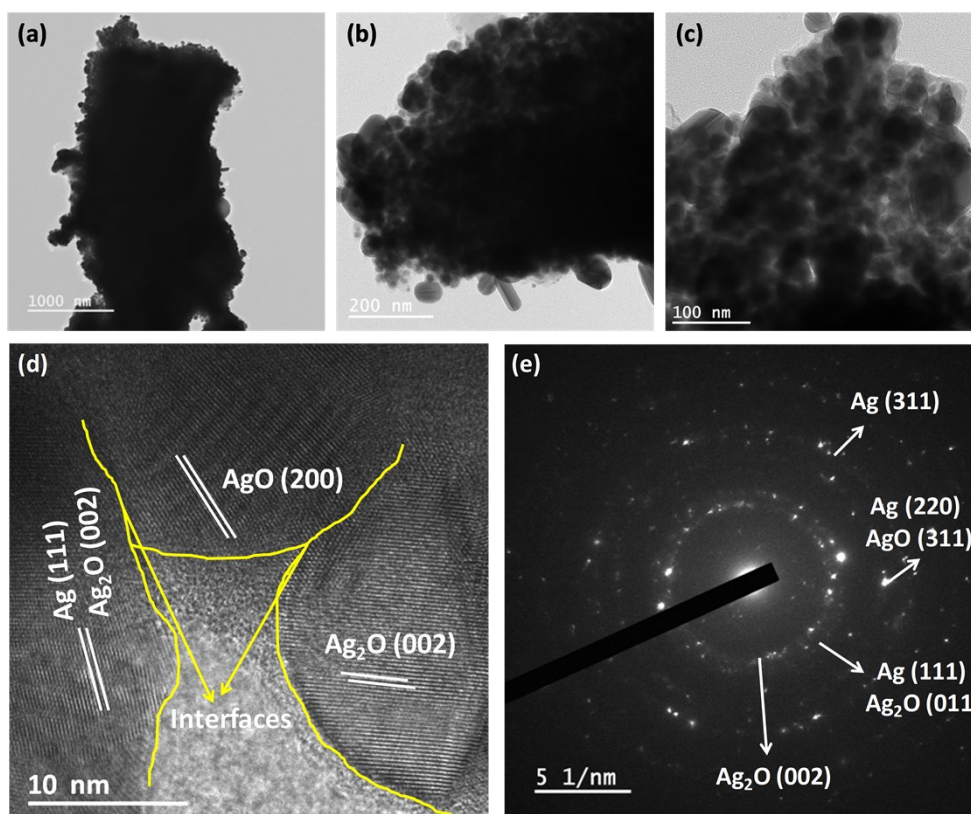


**Figure S5.** (a-c) TEM images, (d, e) HRTEM, SAED images of Ag/AgO<sub>x</sub>-CN<sub>x</sub> after stability.

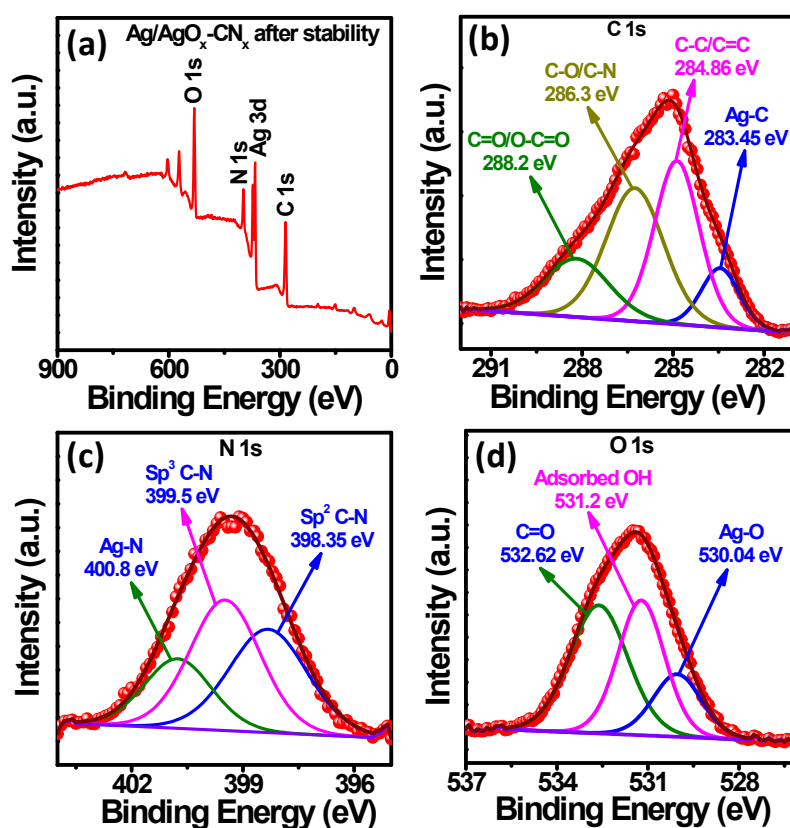


**Figure S6.** (a) XPS survey scan of Ag/AgO<sub>x</sub>-CN<sub>x</sub> after stability, (b-d) High resolution XPS spectrum of C 1s, N 1s, and O 1s, respectively.

**Table S1.** Comparison of HMF oxidation of Ag/AgO<sub>x</sub>-CN<sub>x</sub> with recently published catalysts.

Catalysts	HMF Loading	Electrolyte	Potential (V) and current density (mA/cm <sup>2</sup> )	FDCA Faradic efficiency (%)	Reference
Ag-MOF	10 mM	0.5 M H <sub>2</sub> SO <sub>4</sub>	1.631 V (RHE) at 10 mA/cm <sup>2</sup>	54.2	This work
Ag/AgO <sub>x</sub> -CN <sub>x</sub>	10 mM	0.5 M H <sub>2</sub> SO <sub>4</sub>	1.453 V (RHE) at 10 mA/cm <sup>2</sup>	72.4	This work
NiFe LDH	10 mM	1 M KOH	1.43 V (128.3 mA/cm <sup>2</sup> )	77.2	<i>ACS Catal.</i> 2018, 8, 6, 5533–5541
NiFe LDH	10 mM	1 M KOH	1.23 V (4.6 mA/cm <sup>2</sup> )	99.4	<i>ACS Catal.</i> 2018, 8, 6, 5533–5541
Ni oxide/hydroxides	5 mM	1 M NaOH	1.6 V	84	<i>Electrochim. Acta</i> 1991, 36, 1995-1995
CuO-PdO	50 mM	1 M KOH	~ 1.42 V (RHE) at 20 (mA/cm <sup>2</sup> )	93.7	<i>Adv. Mater.</i> 2022, 34, 2204089
Co(OH) <sub>2</sub> -CeO <sub>2</sub>	10 mM	pH = 7	~ 1.32 V (RHE) at 20 (mA/cm <sup>2</sup> )	85.8% HMFCA yield	<i>Appl. Catal. B: Environ.</i> 2023, 338, 123068
NiS <sub>x</sub> -Ni(OH) <sub>2</sub>	10 mM	1.0 M KOH	~ 1.3 V (RHE) at 20 (mA/cm <sup>2</sup> )	98.3	<i>Adv. Mater.</i> 2023, 35, 2211177
Pt foil	5 mM	0.3 M NaClO <sub>4</sub>	2.1 V	<1% FDCA yield	<i>Catal. Today</i> 2012, 195, 144-154
Au	5 mM	borate buffer (pH 9.2)	1.54 V (< 1 mA/cm <sup>2</sup> )	93	<i>Nat. Chem.</i> 2015, 7, 328-333
PdAu/C	1 mM	5 mM KOH	0.9 V	83% FDCA yield	<i>Green Chem.</i> 2014, 16, 3778-3786
Ni <sub>0.5</sub> Co <sub>2.5</sub> O <sub>4</sub>	50 mM	1 M KOH	~ 1.45 V (RHE) at 20 (mA/cm <sup>2</sup> )	90.35	<i>ACS Catal.</i> 2022, 12, 4242
Ni <sub>2</sub> P	10 mM	1 M KOH	1.423 V (>200 mA/cm <sup>2</sup> )	~ 100	<i>Angew. Chem. Int. Ed.</i> 2016, 55, 9913-9917
Ni <sub>2</sub> S <sub>3</sub>	10 mM	1 M KOH	1.423 V (>200 mA/cm <sup>2</sup> )	~ 100	<i>J. Am. Chem. Soc.</i> 2016, 138, 13639-13646
CoP	50 mM	1 M KOH	1.423 V (>200 mA/cm <sup>2</sup> )	90% FDCA yield	<i>ACS Energy Lett.</i> 2016, 1, 386-390
Pt/Ni(OH) <sub>2</sub>	50 mM	1 M KOH	~ 1.41 V (RHE) at 20 (mA/cm <sup>2</sup> )		<i>Angew. Chem. Int. Ed.</i> 2021, 60, 22908
MoO <sub>x</sub>	20 mM	pH 1 (H <sub>2</sub> SO <sub>4</sub> )	1.6 V	53.8% FDCA yield	<i>ChemSusChem</i> 2018, 11, 2138
MoO <sub>x</sub>	20 mM	pH 1 (H <sub>2</sub> SO <sub>4</sub> )	2.0 V	5.9% FDCA yield	<i>ChemSusChem</i> 2018, 11, 2138
Fe <sub>3</sub> O <sub>4</sub> /Pt/rGO	10 mM	0.05 M H <sub>2</sub> SO <sub>4</sub>	0.6 V vs Ag/AgCl	94.4 % FDCA yield	<i>Catal. Today</i> , 2019, 330, 92-100
CuNi/C	15 mM	1 M KOH	1.45 V	58.8	<i>ChemElectroChem</i> , 2019, 6, 5797-5801
Ru <sub>1</sub> -NiO	50 mM	1.0 M PBS	~ 1.35 V (RHE) at 20 (mA/cm <sup>2</sup> )	70 % FE of DFF	<i>Angew. Chem. Int. Ed.</i> 2022, 61, e202200211
Ni(NS)/CP	5 mM	0.1 M KOH	~ 1.47 V (RHE) at 20 (mA/cm <sup>2</sup> )	99.4% FDCA yield	<i>Angew. Chem. Int. Ed.</i> 2021, 60, 14528
CoAl LDH	10 mM	0.1 M NaOH	0.5 V vs RHE	40.8	<i>J. Mater. Chem. A</i> , 2019, 7, 11241 — 11249
Co-P_DES	15 mM	0.5 M NaHCO <sub>3</sub>	1.45 V	77.3	<i>New J. Chem.</i> , 2020, 44, 14239-14245
Ir-Co <sub>3</sub> O <sub>4</sub>	50 mM	1 M KOH	~ 1.48 V (RHE) at 20 (mA/cm <sup>2</sup> )	98	<i>Adv. Mater.</i> 2021, 33, 2007056



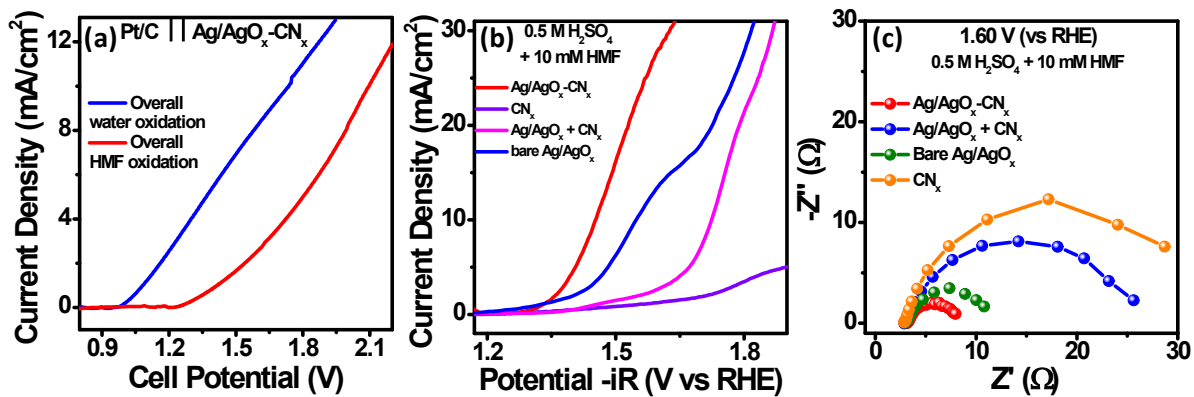


**Figure S7.** (a) Non  $iR$ -corrected overall water and HMF oxidation LSV plots of Ag/AgO<sub>x</sub>-CN<sub>x</sub> by coupling with commercial Pt/C in 0.5 M H<sub>2</sub>SO<sub>4</sub>, (b, c) LSV curves and corresponding nyquist plots of Ag/AgO<sub>x</sub>-CN<sub>x</sub>, bare Ag/AgO<sub>x</sub>, CN<sub>x</sub>, and their physical mixture in 0.5 M H<sub>2</sub>SO<sub>4</sub> solution with 10 mM HMF.